Tenth USA/Europe Air Traffic Management Research and Development Seminar (ATM2013)

Estimating Airspace Capacity Based on Risk Mitigation Metrics

Husni Idris
Engility Corporation
Billerica, MA USA
Husni.idris@engilitycorp.com

Ni Shen
Engility Corporation
Billerica, MA USA
Ni.shen@engilitycorp.com

***Abstract*— Airspace capacity is a key parameter in the air traffic management system. Numerous metrics for estimating it have been proposed including simple ones such as aircraft count and sophisticated ones representing traffic complexity. In this paper, an approach is presented for estimating airspace capacity that addresses two main factors: (1) the risk element in determining capacity, represented by the tradeoff between capacity and the ability to mitigate the risk of violating traffic management constraints, and (2) the cognitive element in determining capacity, represented by the control strategy used by different control schemes such as human control, automation control, or automation assisted control. The approach is demonstrated using a risk mitigation metric, called adaptability, which estimates the number of feasible trajectories that are available to an aircraft, using a certain control strategy, to avoid violating traffic management constraints. Using this metric, the tradeoff between adaptability and capacity to absorb delay that exists in current human control behavior was identified through analysis of historical track data of two airspace sectors. This metric was also used to compare alternative control strategies in a simulated metering situation involving separation assurance and meeting required times of arrival at a fix. The comparison highlighted the higher capacity and adaptability levels that can be achieved with more efficient control strategies relative to human control. Thus, the presented analysis demonstrates the potential of risk mitigation metrics such as adaptability to estimate airspace capacity limits that achieve desired levels of risk mitigation under different control strategies and automation schemes.**

Keywords – airspace capacity; risk mitigation; flexibility; complexity; adaptability; robustness;

I. INTRODUCTION

Capacity is a key parameter in the air traffic management (ATM) system. It needs to be set at values that maintain safe operations and at the same time accommodate the demand for moving passengers in the air transportation system. With the projected increase of the demand for air transportation, properly determining capacity becomes even more critical under the next generation air transportation system (NextGen).

Determining airspace capacity has been a challenging question for the ATM research community. The current measure used for capacity sets a limit on the number of aircraft present in an airspace sector. It is attractive because it is easy to measure but also to control. Over years, many approaches and metrics have been suggested. In a human controlled airspace, traffic complexity often referred to the difficulty of managing the traffic to maintain safe operations. A number of metrics have been suggested for measuring traffic complexity and its limits. Kopardekar and Magyarits listed a number of factors that affect traffic complexity and associated metrics were based on the notion of dynamic density, including, for example, aircraft count and density, sector geometry, traffic mix and distribution, traffic flow structure, mix of aircraft types and performance characteristics, and weather [1][2]. Then using linear regression, factors were found that best correlated with subjective controller ratings of the difficulty to control traffic scenarios of different complexities [3]. Histon et al. [4] and Davison et al. [5] emphasized cognitive elements of complexity, in particular the use of structure by controllers (standard flows, grouping of traffic, and merge points) to simplify the control cognitive processes. Athenes et al. [6] developed a metric that measures the effect of uncertainty and time pressure on controller workload. They used objective measures such as heart rate to demonstrate the validity of their metrics. Delahaye and Puechmorel [7] introduced several complexity metrics based on traffic geometry (proximity, convergence, sensitivity to control maneuver) and traffic flow pattern organization or disorder (topological entropy). They extended the entropy metric building dynamical system models to fit actual aircraft trajectories [8]. Building on this effort, Ishutkina et al. [9] estimated traffic complexity by the ability of a mathematical linear program to interpolate a vector flow field between aircraft positions and velocities, given constraints on speed and turn rate. Aigoin [10] used clustering techniques to measure complexity. Granger and Durant [11] analyzed the impact of the cluster size of aircraft in conflict. Clustering techniques were also used by Billimoria and Lee [12] to determine airspace congestion independent of sectors.

NextGen envisions an ATM system that allocates functions to the human and automation and between different stakeholders such as pilots and controllers in a significantly different manner than today's system. These concepts promise increases in capacity while simultaneously improving safety. For example, in an automation controlled or managed airspace, a computer can perform certain tasks that are needed to separate aircraft and hence the airspace may be able to

This research was funded by NASA under contract NNA11AA44C

accommodate a larger amount of traffic. However, if the automation is turned off the human has to take over and maintain safe separations, possibly with a larger amount of traffic than usually managed by the human and starting from initial patterns that are unfamiliar to the human. In any of these situations, nominal or off-nominal, the airspace capacity has to be set at values that maintain safe operations. A challenge is to develop metrics to estimate airspace capacity that are generic and versatile and hence can be applied to assess the capacity implications of the variety of control schemes envisioned by NextGen as well as practiced in the current environment.

In order to help achieve this goal, in this paper an approach is proposed for estimating airspace capacity that addresses two main factors: (1) the risk element in determining capacity, represented by the tradeoff between capacity and the ability to mitigate the risk of violating traffic management constraints. With a generic metric that captures such risk and the ability of the system to mitigate it, it would be possible to represent human, automation, or mixed operations. (2) The cognitive element in determining capacity, represented by the strategy used to control the traffic situation and mitigate the risk of violating traffic management constraints. The control strategy may represent human control, automation control, or automation assisted control. The control strategy may also represent different schemes of configuring the airspace, structuring traffic flows, distributing functions, among others. Therefore, by explicitly representing the control strategy in the metrics it would be possible to assess and compare the capacity implications of the variety of control schemes envisioned by NextGen as well as practiced in the current environment.

Metrics have been developed to represent the ability of an aircraft trajectory to mitigate the risk of violating traffic management constraints [13][14][15][16] – which was called aircraft trajectory flexibility. These metrics showed promising potential in terms of their generality, conciseness and correlated well with previous metrics of traffic complexity. For example, it was shown in these previous studies that planning aircraft trajectories such that flexibility is increased resulted in mitigating the complexity of the traffic situation. Building on that research, one of these metrics called adaptability was applied in this study to estimate airspace capacity under different control strategies. Using this metric, the tradeoff between adaptability and capacity to absorb delay that exists in current human control behavior was identified through analysis of historical track data of two airspace sectors. This metric was also used to compare alternative control strategies in a simulated metering situation involving separation assurance and meeting required times of arrival. The analysis highlighted the higher capacity and adaptability levels that can be reached with more efficient control strategies relative to human control. Thus, the presented analysis demonstrates the potential of risk mitigation metrics such as adaptability to estimate airspace capacity under different control strategies and automation schemes and to achieve desired levels of risk mitigation ability.

The concept of using risk mitigation metrics to estimate airspace capacity is presented along with the metrics in Section II. Section III presents an analysis of historical traffic data to identify the tradeoff between risk mitigation and capacity under current human control. Section IV compares a human control and an alternative control strategy using simulation. Finally some conclusions and extensions are presented.

II. Concept and Metrics

An approach is presented to estimate airspace capacity based on the ability to mitigate the risk of violating constraints while managing the traffic. Constraints include avoiding violation of the minimum separation requirements and adhering to flow management constraints, which maintain safe operations by avoiding the overload of downstream resources. In this section first the concept of using risk mitigation metrics to estimate airspace capacity is presented. Then airspace capacity metrics and risk mitigation metrics are defined.

A. Using risk mitigation metrics to estimate capacity

Human air traffic controllers attempt to maintain safe operations using conservative methods that reduce the risk of violating ATM constraints to an acceptable level according to their risk tolerance. These methods manifest in the controller decision making strategies while attempting to meet and avoid violating the constraints. These strategies include procedural practices that stabilized over time and resulted in common airspace and traffic structures. They also include dynamic decisions to control continuously changing traffic situations.

Alternative control strategies are often proposed to increase airspace capacity in the face of increasing demand. For example, automated control may adopt strategies to achieve efficiency benefits. Dynamic airspace configurations that are optimized for enhanced aircraft performance may be able to accommodate a larger traffic flow. These new control schemes have to maintain the constraint violation risk below acceptable limits for safe operations as in human control schemes.

Therefore, the amount of traffic that an airspace resource can service – airspace capacity – is dependent on the strategy to control the traffic that the resource services. An automated strategy may be able to serve more traffic than a human control strategy and a structured flow may exhibit higher throughput than a chaotic flow. One method to compare and determine the capacity under different strategies is to relate their capacity to their associated risk of violating constraints. The underlying concept is to determine the capacity levels that can be achieved by alternative control strategies while ensuring an acceptable ability to mitigate the risk of constraint violation. Using this approach, different control strategies can be compared in terms of the tradeoff between capacity and constraint violation risk mitigation. In addition, if a risk mitigation level is desired then such a level may be used to set the airspace capacity limit under each control strategy. In order to instantiate this concept, metrics for measuring airspace capacity and for measuring the ability to mitigate the risk of constraint violation are needed. These metrics are described in the next two subsections.

B. Airspace capacity metrics

Airspace capacity in this paper refers to the ability of an airspace resource, such as a sector, to service air traffic in a traffic flow sense. A number of metrics of the airspace resource can be used to measure this ability such as its maximum

throughput, the maximum delay that can be absorbed in it and the maximum number of aircraft that can be held in it.

Throughput capacity is the maximum flow rate that can be achieved through the airspace resource under infinite demand. It can apply to one or all flow streams through the airspace. Throughput capacity is dependent on the traffic control strategy. For example, higher throughout can be achieved when aircraft travel at faster speeds along shorter paths; when the separation between the aircraft is maintained at lower values; and when different flow streams are parallel rather than crossing. Therefore, increasing the maximum aircraft speed limit and reducing the minimum required separation between aircraft increase throughput capacity.

Some airspace sectors have the capacity to delay aircraft beyond the minimum time that they can spend in the sector. This is desired when congestion at resources downstream of the sector necessitates delaying aircraft before they are released from it. An airspace sector has a limit on the amount of delay that an aircraft can absorb in it depending on its size, the degrees of freedom that are available to absorb delay (for example, speed reduction, path stretching, spinning) and constraints that limit the use of the degrees of freedom such as loss of separation with other aircraft. Therefore, an airspace sector exhibits a delay absorption capacity as the maximum amount of delay that can be absorbed by an aircraft in the sector using a control strategy. For example, a strategy that includes spinning aircraft in a loop enable more lengthening of the path relative to strategies that do not include spinning. Certain tools such as time based metering use the capacity to absorb delay in a sector as a parameter to decide how to allocate delay absorption among sectors along a route of flight.

Similar to delay absorption, an airspace sector may have capacity to hold aircraft. This capacity is the number of aircraft that can be stacked in the airspace with maintaining the minimum separation between them. However, typically the airspace capacity for the number of aircraft is set by the ability of the air traffic controller to monitor and communicate with the same number of aircraft simultaneously. The number of aircraft that can be handled in a sector also depends on the control strategy. For example, the airspace capacity when stacking aircraft using holding patterns is different than when using path stretching only to delay aircraft.

Capacity limits on throughput, delay and aircraft count are related to each other using traffic flow and queuing dynamics. These limits could be computed theoretically under deterministic assumptions and specific traffic flow structures and control strategies. However, practical limits on these parameters are often set lower than theoretical limits based on uncertainties in the environment and the ability of the human controller to control the traffic with acceptable risk. For example, the spacing between aircraft may be increased by a human controller beyond the minimum required to reduce the risk of violating separation constraints. In this study an approach is proposed to identify limits on the airspace capacity metrics based on metrics that measure the ability to mitigate the risk of constraint violation under specific control strategies. These metrics are presented in the next subsection.

C. Risk mitigation metrics

Metrics have been proposed by the authors to represent the exposure of the aircraft to the risk of violating constraints imposed on it using a decision theoretic approach [13][14][15][16]. Using the decision theory approach the solution space of an underlying control strategy was represented by a discrete decision tree. ATM constraints were incorporated into the decision tree resulting in the elimination of infeasible solutions that violate the constraints. Based on counting the feasible and infeasible solutions, metrics for measuring the ability to mitigate the risk of violating the constraints were derived and extended for this study as follows.

Constraints are imposed on aircraft trajectories to meet certain objectives, such as imposing a required time of arrival (RTA) which is intended to help balance demand and capacity of airspace resources. Constraints are also imposed on trajectories in order to avoid safety hazards, such as violation of separation requirements from traffic or weather cells. The violation of the constraints may be caused by uncertainties in the constraints, which were called constraint disturbances; they represent variation in predicted constraints or appearance of new constraints that were unforeseen at the time of trajectory planning. The violation of constraints may also be caused by uncertainties in the aircraft states, which were called state disturbances; they represent predicted or unforeseen deviations in the state due to wind or pilot error for example. Flexibility of the aircraft trajectory was defined as its ability to mitigate the risk of constraint violation. The following characteristics were defined to help derive metrics for measuring this risk.

Robustness (RBT) is defined as the ability of the aircraft to maintain feasibility (i.e., not violating any constraints) despite the occurrence of constraint and state disturbances that pose the risk of constraint violation. Robustness, denoted as RBT, is measured with the probability of feasibility RBT(.) = Pf(.), where the dot refers to the object of which robustness is measured. Hence, the robustness of a specific aircraft trajectory is defined as the probability that the trajectory remains feasible. For example if the trajectory (traj) is defined as a series of points (k) in space and time, and each point has a probability of feasibility pf(k) that is independent of all other points, then the probability of feasibility of the trajectory is the multiplication of the independent probabilities of feasibility of all the trajectory points: RBT (traj) = Pf(traj) = Π_k(pf(k)). The robustness of the solution space that consists of a set of possible trajectories available to the aircraft at a point (k) and that the aircraft can select from according to a decision strategy is defined as the probability that a trajectory selected according to the strategy is feasible. For example, one decision strategy is to select a trajectory out of the total trajectories available at a point (k) randomly (i.e. with equal probability) regardless of the outcome of disturbances. Using this simplified decision strategy, Idris showed that the probability of feasibility of the selected trajectory at any point k (i.e., RBT at point k) can be estimated by the ratio of the expected number of feasible trajectories f(k) to the expected total number of trajectories N(k) available at the point k [13]. RBT(k) = Pf(random traj selected at k) = f(k) / N(k) where N is the sum of feasible and infeasible trajectories and the number of trajectories are expected values given the disturbance probability distributions.

Adaptability (ADP) is defined as the ability of the aircraft to regain feasibility of its trajectory in case it lost it due to the occurrence of disturbances. The aircraft regains feasibility by selecting from the feasible trajectories available to it at that point in space and time according to a decision strategy. Therefore, adaptability at a point in space and time (k), is measured with the expected number of feasible trajectories f(k) available to the aircraft to select from according to a decision strategy: ADP(k) = f(k), where f(k) is the expected value given the probability distributions of the disturbances.

In order to measure robustness and adaptability as defined above, the number of total and feasible trajectories available to the aircraft at a point k in space and time to reach its destination needs to be estimated. The destination is a collection of points in space and time representing, for example, an RTA at a fix with some temporal or spatial tolerance. To be able to count the number of trajectories, a discrete representation of time and space and of the solution space is developed as follows:

- Time is discretized into equal time steps (ε apart) up to a time horizon T, representing for example the RTA.
- The airspace available is discretized into rectangular cells in three dimensions (or two if planar).
- The number of trajectories is estimated at the center (k) of each cell at each of the time steps. Therefore the sizes of the time steps and of the spatial cells represent the estimation sampling resolution.
- The aircraft degrees of freedom (speed, heading, and altitude) assume discrete values between maximum and minimum limits. Their limits and resolutions may represent operational procedures, human behavior, or decision strategy. For example speed may be allowed to change in increments of five km/hour only. The limits and resolutions may be different depending on the point k in the time-space domain and the aircraft state in terms of speed, heading and altitude at k.
- Each trajectory is assumed to consist of a series of the discrete cells k that are reachable given the aircraft degrees of freedom and the assumption that the values of the degrees of freedom are maintained constant between two successive time steps.
- Reachability is measured from the centers of the cells, which are the points k at which the number of trajectories are estimated. A cell is considered reachable from a cell in the previous time step if any part of it is reachable given the assumption of constant values of the degrees of freedom along the time step. The number of ways a cell can reach another cell in the next time step are counted and recorded in the reachability function g(k). This is depicted on the left side of Fig. 1 for a two dimensional example with three heading values and three speed values. The cells that are reachable from the center of a cell (k) with coordinates (11, 11) over one time step are identified. The values of the function g(k) are noted on each cell that has a value larger than zero. The right hand side of Fig. 1 shows the process repeated to compute the reachability function from the centers of the reachable cells over the next time step. In this example the function g(k) was assumed the same for all cells, but it can be dependent on k and the speed and heading at k.
- The example shown in Fig. 1 is deterministic, where each of the reachable points that lie within a cell occurs with probability of one. To represent state disturbances, each of these points may be substituted with multiple reachable points with a probability value assigned to each. Then an expected number of trajectories that reach a cell can be computed.

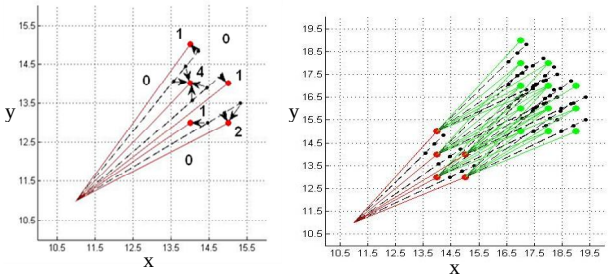

Figure 1. Example of discrete framework and reachability from one cell

A method for estimating the metrics has been devised, as described in Idris et al [16]. The method estimates the number of trajectories that emanate from each of the cell centers k to the destination. It combines a convolution process to count the number of trajectories in the discrete reachability tree with a filtering process to eliminate infeasible trajectories that violate constraints. It is summarized in the following steps and depicted in Fig. 2 for a two dimensional case:

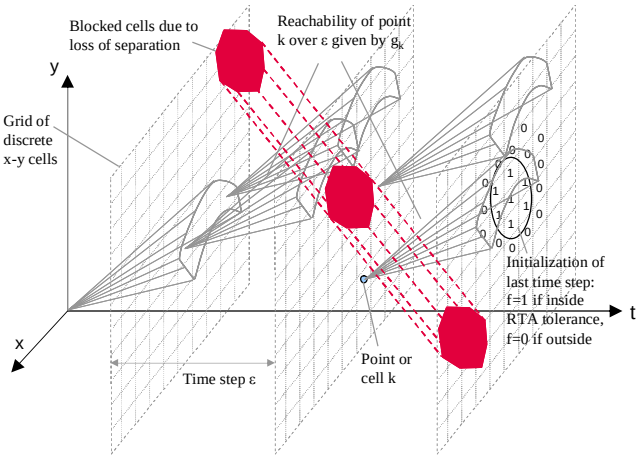

Figure 2. Discrete estimation of number of feasible trajectories

1. First, the last time step T is initialized by setting the number of trajectories $f_T(k)$ to one for each cell k that is feasible and to zero for each cell k that is not. Feasibility is determined based on constraint violation. If the center of the cell violates separation with another aircraft, or lies within a hazard airspace, or lies outside a required time-space region, then it is infeasible. In

Fig. 2, the cells that lie within an RTA requirement are set to one and the ones that violate it to zero. Also in Fig. 2 the trajectory of an intruder aircraft (or weather polygon) is enclosed in a polyhedral object (shown in red) that represents the separation requirements from it. The resulting polyhedral object eliminates certain volume of the solution space. A center of a cell that lies inside the polyhedral object indicates infeasibility of the cell and its f_T is set to zero.

2. The reachability function g(k) is computed for each cell in the previous time step T-1. This results in $g_{T-1}(k \rightarrow i)$ – the number of trajectories that reach from each cell k in time step T-1 to each cell i in time step T.
3. If the trajectory segment connecting the center of cell k in time step T-1 and the center of cell i in time step T is not feasible, the corresponding value $g_{T-1}(k \rightarrow i)$ is set to zero. The segment may not be feasible if violating separation with another aircraft, crossing a hazardous airspace, or violating an RTA. In Fig. 2, the segment is infeasible if it crosses the red polyhedral object representing an intruder aircraft trajectory.
4. Then the function $g_{T-1}(k)$ is multiplied by the function $f_T(i)$ of the last time step T to compute the number of feasible trajectories $f_{T-1}(k)$ at each cell k in the previous time step: $f_{T-1}(k) = \sum_i \{g_{T-1}(k \rightarrow i) \times f_T(i)\}$.
5. Steps 1 through 4 are then repeated for the previous time steps, replacing T with T-1 and T-1 with T-2, until the initial state is reached.

Given this discrete representation of the trajectory solution space, a number of metrics representing risk of constraint violation can be formulated. For example, RBT, ADP, or combinations of them have been used in previous analyses. In the analysis in this paper the adaptability metric ADP was used.

III. Capacity-Risk Tradeoff under Current Human Control Strategy

In this section the method presented in the previous section is applied to a human control strategy elicited through interview with an experienced controller. First the control strategy is described followed by an analysis of the tradeoff between capacity and risk mitigation in two airspace sectors.

A. Human control strategy

The following notes describe human strategies involving metering situations. The process of merging and sequencing the aircraft in a stream that feeds a meter fix involves a low altitude sector ending at the fix and one or two high altitude sectors that feed the low altitude sector. For simplicity we assume one low and one high sector. The controllers of the low and high sectors attempt to absorb the delay displayed by a scheduler for each flight. Their procedures and behavior depend on the amount of delay that needs to be absorbed as outlined in Table 1.

A human controller typically simplifies the solution space to few degrees of freedom by a number of techniques. This simplification is due to the limited ability of the human controller to process a large number of degrees of freedom for a large number of aircraft. One simplification technique is grouping the aircraft into a "string" of platooning aircraft. This reduces the degrees of freedom to the length of the string as opposed to the combinations of the heading, speed and altitude degrees of freedom of all aircraft. Namely, the controller has only to manage the length of the string in order to absorb delay while keeping the aircraft separated along the string.

TABLE I. HUMAN CONTROL STRATEGY IN METERING SITUATION

Delay	High sector	Low sector
1 to 2 minutes	Do nothing	Drop speed to 491 then to 463 km/hr (265 to 250 knots)
3 minutes	Do nothing	Use path stretch
4 to 7 minutes	Drop speed to 463 km/hr (250 knots). Establish a sequence. Drop altitude earlier to level 270, to give low sector more control at low altitude	Use path stretch. For larger delay drop altitude earlier to level 190, to allow more control at low altitude, increasing level segment at 190
More than 7 minutes	Descend to altitudes stacked by 300 meters (1000 feet) anticipating holding	Hold aircraft. The exit from the holding pattern is computed to meet the time at fix

This situation is depicted in Fig. 3 where a string of aircraft is shown. A path stretch is performed close to the meter fix for small delay and grows upstream as the delay needed is larger. According to the interview, one reason for absorbing the delay near the meter fix is to avoid committing the delay too early anticipating that the delay requirement may be withdrawn. Another reason is that the aircraft are "lower and slower" near the meter fix giving the controller more controllability.

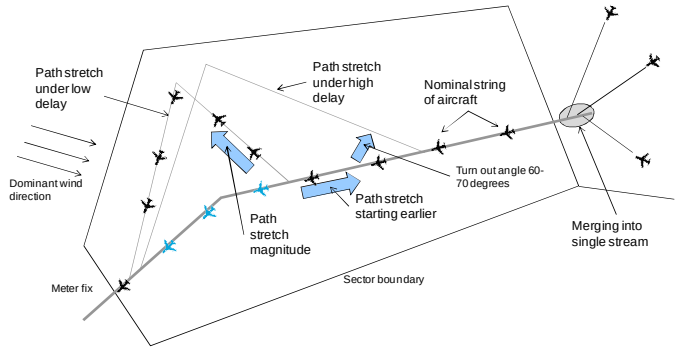

Figure 3. Human path stretch strategy in metering situation

The basic variables that are controlled to stretch the string of aircraft as more delay absorption is needed are the start of the deviation from the center line, the magnitude of the deviation, and the turn out angle. The extent of the deviation is determined by the widest area of the sector, as shown in Fig. 3. According to the interview, the controller is able to compute the appropriate turn back point to meet the RTA with one minute tolerance. If increasing the path stretch magnitude is not enough, the starting point is moved upstream to start the delay

absorption earlier. Throughout the process the string of aircraft remains intact. The turn-out angle may also be increased, but according to the controller interview, stays below 60-70 degrees. Turning is typically performed only to the larger side of the sector where there is more space to path stretch. While S-turns using both sides may be practiced, they are rare. The turn angle is typically against the dominant wind direction as indicated in Fig. 3. When the wind direction changes dynamically, the turn direction is based on the sector geometry and space availability as opposed to wind direction.

B. Tradeof between Risk mitigation and capacity

Two sectors that feed arrival gates of the Chicago O'Hare airport (ORD) were selected for analysis because their traffic flow patterns represented the elicited decision strategy described in the previous subsection. The two sectors included a small size sector ZAU26 and a relatively large sector ZAU74. In particular, both sectors merge the inbound traffic to a center line that exits the sector at a fix and both sectors perform path stretch to predominantly one side. This is shown in the flight plans in Fig. 4 for both sectors and in the actual trajectories from one day (ASDI June 7, 2004) in Fig. 5.

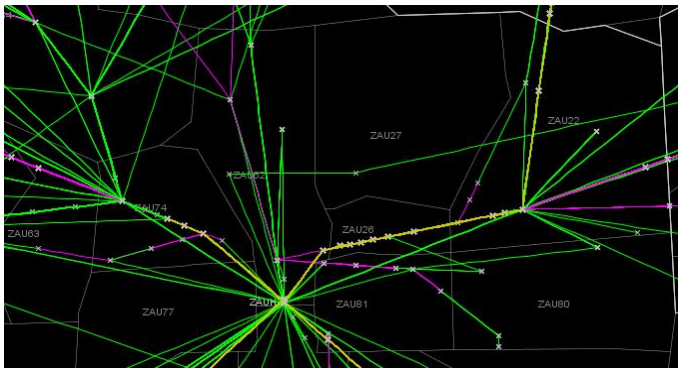

Figure 4. Flight plans for sectors ZAU74 and ZAU26

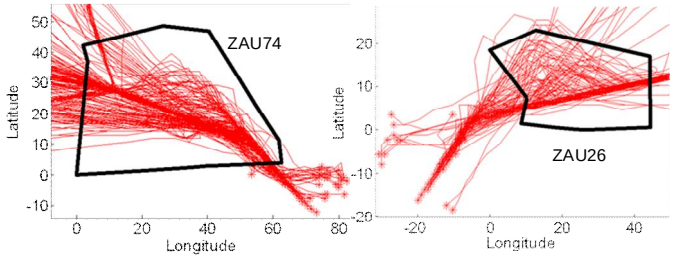

Figure 5. Actual trajectories showing pathstretch in ZAU74 and ZAU26

As seen in the flight plan and the actual trajectories in the figures, the general behavior is to merge the traffic in a single stream. In the case of the smaller sector ZAU26, the merge is mainly performed in an upstream sector ZAU22 while ZAU26 mainly meters the traffic through path stretching. In the case of the larger sector ZAU74, the traffic is merged within the sector then path stretch is performed mainly after the merge. While there are some dominant merge points, the merge seems to occur sometimes loosely throughout the centerline.

As described in Table 1, the air traffic controller switches to holding aircraft when the delay is larger than a certain value, typically around six or seven minutes. Fig. 6 shows the traffic trajectories from another day of operations for each of the sectors ZAU26 and ZAU74 when the delay was higher than the examples shown in Fig. 5. The loops that are evident in the track data indicate that the dominant strategy to absorb delay used by the air traffic controllers in these cases was holding.

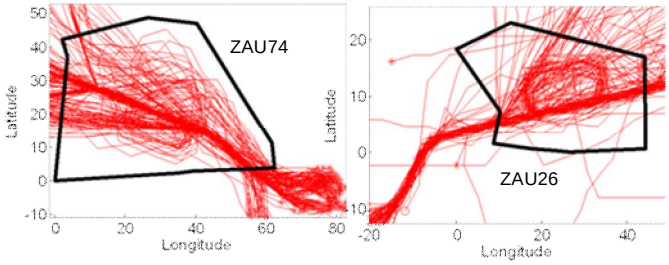

Figure 6. Actual trajectories showing holding in ZAU74 and ZAU26

ADP versus delay curves were generated for the two sectors ZAU26 and ZAU74 using ASDI traffic data from May and June of 2004. For each flight that passed through the sectors heading to ORD, delay and ADP were computed as follows. The entry and exit points were determined as the crossings of the sector boundary using extrapolation of track data if needed. The duration of the flight in the sector was taken as the exit time minus the entry time. The delay was computed by subtracting from the duration an unimpeded travel time, taken as the travel time over a straight line between the entry and exit points using the entry speed of the aircraft. In order to isolate the flights that were delayed using path stretching, aircraft that were held were identified using an algorithm that detected a loop in the trajectory. Fig. 7 shows two delay histograms for each sector, where each flight is one occurrence: one for the sample with all flights and one for flights that were not held. The two frequencies are similar at low delay values as expected because no holding was applied at low delay. As delay grows, the number of flights that were held grows relative to the total.

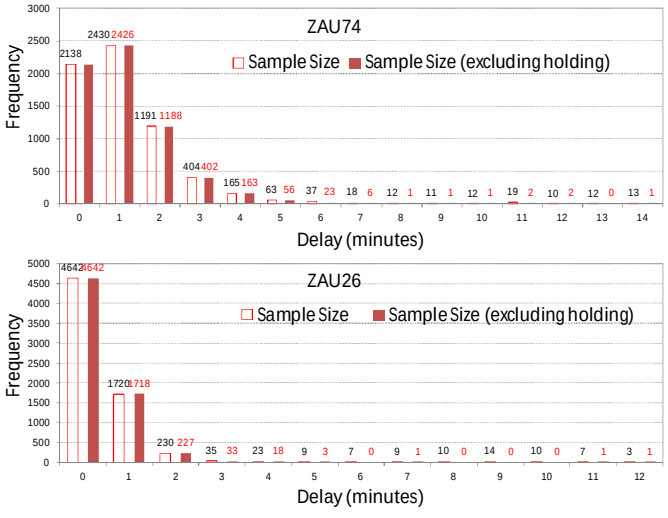

Figure 7. Delay distrubution in ZAU74 and ZAU26

The adaptability metric ADP was computed for each flight using the method presented in Section II.C. The discrete

solution space representing the underlying human control strategy was generated for the flight using the following assumptions and ADP was taken as the number of feasible trajectories at the starting point (entry point into the sector):

- Each flight was required to spend in the sector the duration computed from the actual data.
- Each flight merged on the center line between the dominant entry and exit points in the flight plans (see Fig. 4). The flight can merge anywhere along the center line as was inferred from the actual data.
- The flight used path stretch to one side only, as determined in Fig. 5. Path stretch starts after the merge.
- The aircraft was forced to return to the exit point along the center line before exiting the sector. A tolerance of 5.6 km (three miles) around the exit point was used.
- The aircraft was allowed to step down its speed using three values inferred from the actual data. The ground speed reported in the ASDI data was analyzed to determine the three dominant speeds, where each report was used as an occurrence (See Fig. 8 for an example). A large bin size of 93 km/hr (fifty knots) was used to categorize speed in mostly three values.
- Altitude was ignored in this analysis. Hence the speed reduction represented speed reduction due to descent as well as commanded speed reduction to absorb delay.
- Flights not destined to ORD were considered intruder aircraft and their trajectories blocked some of the solution space of the ORD flights thus reducing the number of feasible trajectories in ADP. 9.3 km (Five miles) were used as the minimum separation required.

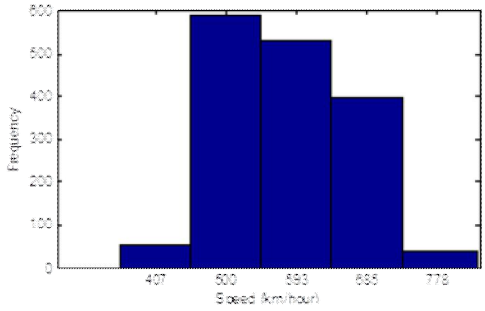

Figure 8. Example of speed distribution to identify dominant speeds

Fig. 9 shows the ADP versus delay plots for the two sectors analyzed. The log of ADP is plotted on the vertical axis and the delay that was required on the horizontal axis. ADP was averaged over the flights in each delay bin, excluding the flights that were held because they used a different strategy to absorb delay than path stretching. The flights that were held are encircled in the figure. The values of the log of the average ADP at each delay bin are connected to show the overall trend. At low delay values the ADP value is small because as the required duration approaches the unimpeded duration (i.e. zero delay), there are few solutions for the aircraft to meet it. As the delay increases the ADP value also increases reflecting more solutions available to meet the corresponding durations. The average ADP value reaches a maximum indicating that adaptability, and hence the ability to mitigate the risk of constraint violation, is highest at certain delay values larger than zero. This indicates that forcing some aircraft to spend more than their unimpeded travel time in the sector allows the controller to adapt to possible risks of violating constraints, including in this case the imposed delay. Then ADP starts to decline as the number of feasible solutions to meet higher values of delay, using path stretching, becomes smaller. This trend is the same for both sectors, with the smaller sector exhibiting smaller ADP values because of its smaller size. The kinks in the trend are due to the smaller sample at higher delay.

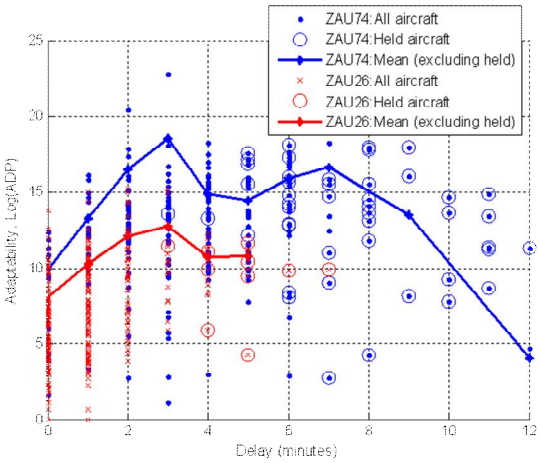

Figure 9. Adaptability (ADP) versus delay tradeoff

There is a wide variation in the values of ADP at each delay bin in Fig. 9. Two main sources of this variation are the number of intruder traffic and the distance between the entry and exit points. Fig. 10 shows the correlation of ADP with the number of intruder aircraft, for one duration (13 minutes), in sector ZAU74 as an example. As expected, ADP is smaller the larger the number of intruder aircraft, because the intruder traffic eliminates trajectories that violate the minimum separation.

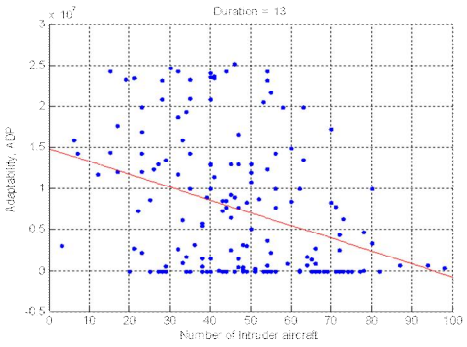

Figure 10. Adaptability (ADP) versus number of intruder aircraft

The ADP versus delay analysis in Fig. 9 was conducted using flights that were path stretched or slowed down to absorb delay rather than held using spinning. As the required delay increases the air traffic controllers switch from using path stretch to using holding as the delay absorption strategy.

Therefore, switching to holding can be used as an indication of reaching or exceeding the capacity to absorb delay using path stretch, as perceived by the air traffic controller. In order to identify this capacity limit, the percentage of flights that were held was plotted at each of the delay values. The holding rates are superimposed on the ADP versus delay curves for the two sectors that were analyzed, as shown in Fig. 11. The holding rate is zero at low delay values then it starts increasing at some delay value and reaches hundred percent at high delay values. As expected, holding starts earlier for the smaller sector ZAU26 because it has less capacity to absorb delay using path stretch than the larger sector ZAU74. For sector ZAU26, holding started at about three minutes of delay, reached fifty percent around five minutes and reached hundred percent at about six or seven minutes of delay. For sector ZAU74 holding was at ten percent at a delay value of about five minutes, reached fifty percent around seven minutes and reached ninety percent around eight minutes. It should be noted that the sample size gets small at high delay values as was shown in Fig. 7, making it difficult to estimate when holding reached hundred percent because of noise.

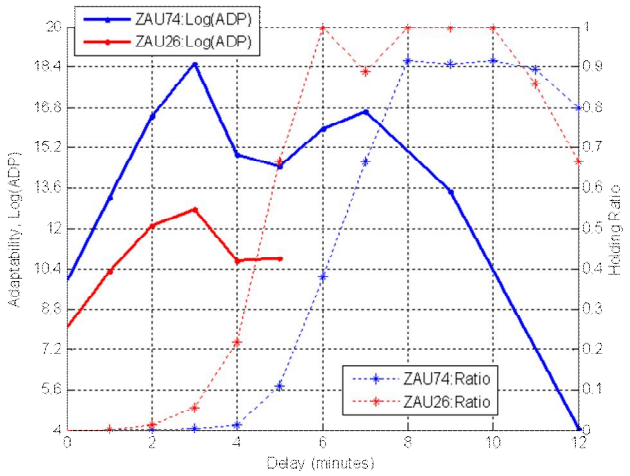

Figure 11. Path strecth delay capacity limit as indicated by holding

Switching to holding is used as an indication of the controller's perception of the sector capacity to absorb delay using path stretch. Hence, one can read in Fig. 11 the ADP values at the capacity limits of absorbing delay using path stretch where the controller switches from path stretching to a holding strategy. One can also infer what ADP values were considered acceptable by the controller at such capacity limits for each sector. For example, using fifty percent holding as a threshold indication of strategy switch, the corresponding log-ADP value for the smaller sector ZAU26 is around 10 while for the larger sector ZAU74 is around 15.

The two sectors analyzed indicate that the level of ADP that corresponded to capacity to absorb delay using path stretch as perceived by the controller (i.e., switching to holding) depended on the sector size. This observation may have a number of reasons. For example, one observation is that the smaller sector ZAU26 used almost all of the area of the sector for path stretching while the larger sector ZAU74 used less of its complete area (see Fig. 5). The ADP metric in this analysis assumed that all of the sector area is available for path stretch solutions. Hence, the ADP values for ZAU74 may have overestimated the number of feasible solutions compared to what the controller considered an available area for solutions. The air traffic controller may switch to holding at certain delay values for which path stretching becomes excessive, even if additional sector area is still available to perform larger path stretches to absorb larger delays. It should be noted that this observation is based on analysis of two sectors only; a wider analysis is needed to generalize this observation and identify additional insights about inherent human capacity perception.

IV. Capacity-Risk Tradeoff under Alternative Control Strategies

In this section an analysis demonstrates how alternative control schemes can be compared using the risk mitigation and capacity metrics presented in Section II. As an example, the human control strategy described in Section III is compared to another control strategy, assumed to be used by automation, in terms of the tradeoff between capacity represented by the limit to absorb delay and risk mitigation represented by ADP.

An algorithm based on the Efficient Descent Advisor (EDA) decision support tool was used as an example of an automation control strategy to absorb delay [17]. The algorithm absorbs delay in a metering situation by considering each aircraft individually without coupling the aircraft along a string. See Fig. 12. EDA uses speed as the preferred degree of freedom to absorb delay and if insufficient it resorts to path stretching. The trajectories generated are conflict free. The premise of the automation is to absorb the delay needed at higher altitude enabling more efficient continuous descent. The human controller would be unable to compute the types of solutions that the automation computes; hence would not reap such benefits. The automation strategy would also use the airspace more effectively. Whereas the airspace is reduced in the human control case to a stretched string of aircraft, the automation is able to spread the aircraft more effectively.

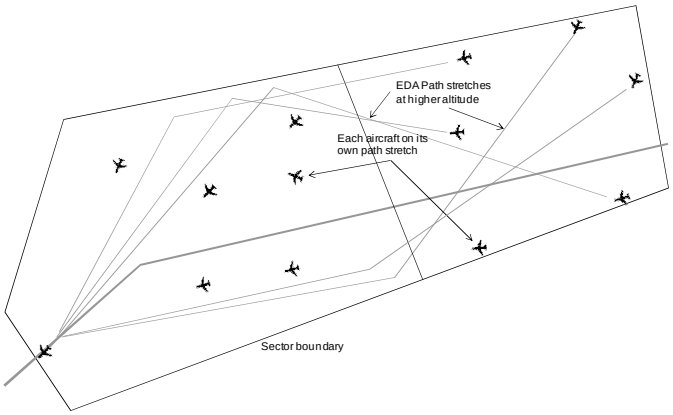

Figure 12. Alternative path stretch strategy in metering situation

The human and automation control strategies described in Fig. 3 and Fig. 12 respectively, were simulated in a Matlab environment using the discrete space-time decision tree described in Section II.C with the same parameters except for differences in the control strategy. A hypothetical two

dimensional airspace was modeled as a 185 km by 278 km (100 by 150 nautical mile) rectangle as shown in Fig 13, with a resolution of 185 meter (one nautical mile) square cells. Time was discretized into one minute increments. The centerline of the flow starts at point (0, 0) and ends at the metering fix at point (0, 150). Aircraft were introduced at random locations along an arc centered about the meter fix, which ensures that all flights are equidistant from the metering fix when they enter the airspace to reduce variability. Each aircraft was required to absorb a delay which was varied in the simulation experiment to determine the capacity of the airspace to absorb delay.

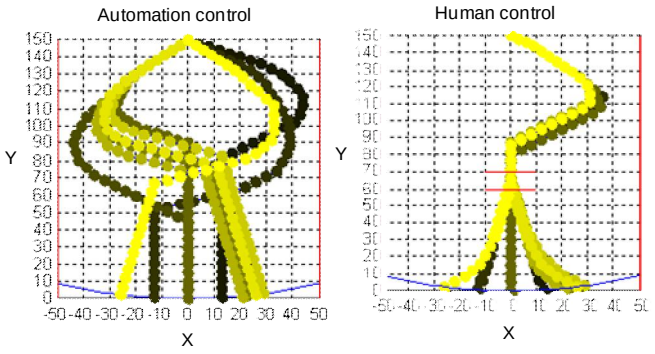

Figure 13. Simulation of human and automation control strategies

The differences of the automation from the human control assumptions described in Section III.B are: (1) aircraft were not forced to merge on the centerline, rather were allowed to path stretch from their entry and (2) path stretching was allowed to both sides of the centerline as shown by example trajectories in Fig. 13. In both strategies aircraft were allowed to reduce speed using 556, 500, 445 km/hr (300, 270, 240 knots) steps.

A steady state condition was analyzed for both the human and automation control cases, where the rate of aircraft entry into the airspace was set to be equal to the rate at which the aircraft exited the airspace. Ten aircraft were introduced two minutes apart and forced to leave at the meter fix also two minutes apart. Under such a condition the number of aircraft in the airspace does not grow dynamically, and the amount of delay that is absorbed in the airspace corresponds to the number of aircraft in it. Each aircraft was assumed to follow a trajectory that was generated by optimizing ADP using a dynamic program. This trajectory was assumed to be known to the other aircraft and was taken into account in the computation of ADP as described in Section II.C. Therefore ADP for each aircraft counted the number of feasible trajectories that did not lose separation with the trajectories of preceding aircraft.

For both the human and automation control strategies, increasing values of delay were imposed on all ten aircraft until no solution was possible, indicating reaching the delay absorption capacity using each strategy. In this analysis, the airspace capacity was measured in terms of the maximum ability to absorb delay at constant throughput. A similar analysis can be conducted for identifying the maximum throughput that can be achieved. ADP was computed for each aircraft at its initial position and averaged over all aircraft. Fig. 14 plots the log of the average ADP value versus the required delay. The following observations can be made from the figure.

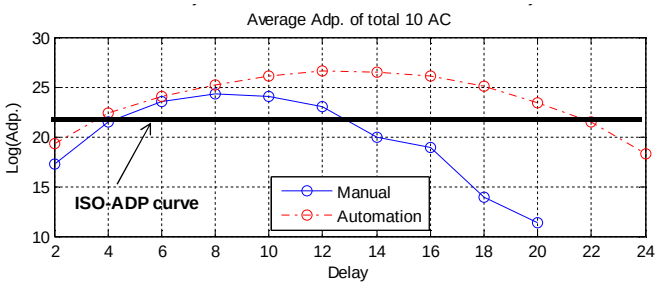

Figure 14. Adaptability vs delay for human and automation control strategies

Fig. 14 shows that the automation strategy was able to absorb more delay because of the increase in the degrees of freedom relative to the human control strategy modeled. Namely, the aircraft can path stretch earlier and to either side of the centerline. Therefore, under this automation strategy it was possible to absorb 24 minutes of delay, by all ten aircraft, while the human control strategy was able to absorb a maximum of 20 minutes of delay, with the same airspace size.

Each ADP versus delay curve in Fig. 14 shows the same tradeoff between adaptability and capacity to absorb delay that was observed in the historical data analysis in Fig. 9. Namely, each curve exhibits a limited capacity to allow unimpeded travel (zero delay) as ADP is low at low delay values. (Note that although not shown in Fig. 14, log(ADP) is equal to zero at zero delay because there is only one solution corresponding to the fastest transition time.) Each curve reaches a limit on the capacity of the airspace to absorb high delay values as ADP drops to low values and ultimately zero. The curves also show that adaptability reaches a maximum level at certain delay values that are higher than zero. This indicates that forcing aircraft to spend more than their unimpeded travel time in the sector allows the control strategy to adapt better to possible risks of violating constraints, including in this case the imposed target throughput of two minutes between aircraft.

While the theoretical capacity to absorb delay corresponds in Fig. 14 to where ADP drops to zero, practical limits are usually set at higher ADP values, as was demonstrated in the previous section where human controllers switched from path stretching to holding aircraft at relatively high ADP values. Fig. 14 depicts a horizontal ISO-ADP line that represents notionally such an adaptability threshold that is larger than zero. This threshold may represent either inherent risk tolerance (as in a human controller) or a desired level of risk mitigation that should be afforded by either human, automation, or combined control strategies. Using the analysis approach presented in the previous section, albeit applied to a larger number of sectors, one may infer statistically levels of adaptability that the human controller considers acceptable under certain conditions and control strategies. The identification of a desired adaptability level under human or automation control is a subject of further research and would consider safety standards for example. Given the existence of such a desired ADP level, it can be used to trace the delay limits that produce this ADP level under the different control strategies as shown by the ISO-ADP line in Fig. 14. For example, this line demonstrates that at the same adaptability, or risk mitigation level, higher delay absorption capacity may be

reached with the automation strategy, by generating more solutions, which is one benefit of automation.

Another observation from Fig. 14 is that the adaptability ADP is higher, particularly at higher delay values, under the automation control strategy. Therefore, for the same delay requirement, the additional solutions considered by the automation enable more mitigation of the risk of violating constraints. It should be noted however, that while the automation is capable of considering these additional solutions, the human may not be able to. Therefore, if the automation failed, the human has to handle using human control strategies more traffic and unusual traffic patterns that the automation was handling. Hence the human controller may not achieve the same level of adaptability or risk mitigation as the automation. The approach presented in this paper may be applied to such off-nominal conditions to assess the risk mitigation that the human may experience when taking over from automation.

V. Conclusions and Future Extensions

A risk mitigation metric called adaptability was applied to analyze the tradeoff between risk mitigation and airspace capacity under different control strategies that may represent current or future control schemes. By analyzing historical traffic data, it was possible to identify the tradeoff between adaptability and capacity to absorb delay that is inherent in human control strategies using path stretch in metering situations as an example. It was shown that the human controller switched from path stretching to holding aircraft at relatively high values of adaptability where there were still solutions to absorb delay using path stretch, particularly in a larger sector. A human control strategy was also compared to an alternative strategy, representing automation for example, demonstrating the potential of metrics such as adaptability to determine capacity limits at desired levels of risk mitigation. The analysis presented is preliminary with many possible extensions. For example, research may be conducted to relate the presented risk mitigation metrics to safety and to analyze a larger set of airspace resources and control strategies to generalize the insights about human risk tolerance and capacity perception. In addition, the metrics can be applied to assess future ATM control schemes, in nominal and off-nominal conditions, in terms of risk mitigation and capacity tradeoffs.

Acknowledgment

The authors thank Larry Myen, Karl Billimoria, Nancy Smith and Paul Lee of the NASA Ames Research Center and Greg Dyer of the FAA Denver Control Center.

References

[1]. P. Kopardekar and S. Magyarits, “Measurements and prediction of dynamic density,” Proceedings of the 5th USA/Europe Air Traffic Management R&D Seminar Budapest, Hungary, 2003.

[2]. I. V. Laudeman, S. G. Shelden, R. Branstrom, and C. L. Brasil, “Dynamic density: an air traffic management metric,” 1999, NASA-TM-1998-112226.

[3]. B. Sridhar, K. S. Sheth, and S. Grabbe, “Airspace complexity and its application in air traffic management,” Proceedings of the 2nd USA/Europe Air Traffic Management R&D Seminar, Orlando, Florida, 1998.

[4]. J. M. Histon, G. Aigoin, D. Delahaye,R. J. Hansman, and S. Puechmorel, “Introducing structural considerations into complexity metrics,” Proceedings of the 4th USA/Europe Air Traffic Management R&D Seminar, Sante Fe, NM, 2001.

[5]. J. Davison, J. Histon, M. Ragnarsdottir, L. Major, and R. J. Hansman, "Impact of operating context on the use of structure in air traffic controller cognitive processes,” Proceedings of the 5th USA/Europe Air Traffic Management R&D Seminar Budapest, Hungary, 2003.

[6]. S. Athenes, P. Averty, S. Puechmorel, D. Delahaye, and C. Collet, “ATC complexity and controller workload: trying to bridge the gap,” HCI-Aero 2002 International Conference on Human-Computer Interaction in Aeronautics.

[7]. D. Delahaye and S. Puechmorel, “Air traffic complexity: towards intrinsic metrics,” Proceedings of 3rd USA/Europe Air Traffic Management R&D Seminar, Napoli, Italy, 2000.

[8]. D. Delahaye, S. Puechmorel, R. J. Hansman, and J. Histon, “Air traffic complexity based on non linear dynamical systems,” Proceedings of the 5th USA/Europe Air Traffic Management R&D Seminar, Budapest, Hungary, 2003.

[9]. M. Ishutkina, E. Feron, and K. Billimoria, “Describing air traffic complexity using mathematical programming,” AIAA-2005-7453.

[10]. G. Aigoin, G. “Air traffic complexity modeling,” Master Thesis. ENAC: France.

[11]. G. Granger and N. Durand, “A traffic complexity approach through cluster analysis,” Proceedings of the 5th USA/Europe Air Traffic Management R&D Seminar, Budapest, Hungary, 2003.

[12]. K. Billimoria and H. Lee, “Analysis of aircraft cluster to measure sector-independent airspace congestion,” AIAA 2005-7455, 2005.

[13]. H. Idris, R. Vivona, and D. Wing, “Metrics for traffic complexity management in self-separation operations,” Air Traffic Control Quarterly, Volume 17, Number 1, 2009.

[14]. H. Idris, D. Delahaye, and D. Wing., “Distributed trajectory flexibility preservation for traffic complexity mitigation,” Proceedings of the 8th USA/Europe Air Traffic Management R&D Seminar, Napa valley, California, 2009.

[15]. H. Idris, N. Shen, T. El-Wakil, and D. Wing, “Analysis of trajectory flexibility preservation impact on traffic complexity,” Proceedings of the AIAA Guidance Navigation and Control Conference, AIAA-2009-6168, 2009.

[16]. H. Idris, N. Shen, and D. Wing, “Complexity management using metrics for trajectory flexibility preservation and constraint minimization” Proceedings of the AIAA Aviation Technology, Integration, and Operations Conference, 2011.

[17]. R. A. Coppenbarger, R. Lanier, D. Sweet, and S. Dorsky, "Design and Development of the En Route Descent Advisor (EDA) for Conflict-Free Arrival Metering," AIAA-2004-4875, AIAA Guidance, Navigation, and Control Conference, Providence, RI, 2004.

Author Biography

Husni Idris received a bachelor of science (1989) and a master of science (1992) in mechanical engineering, a master of science in operations research (2000) and a Ph.D. in human factors and automation (2000), all from the Massachusetts Institute of Technology, Cambridge, Massachusetts, USA. He is a Principal Research Engineer at Engility Corporation, Billerica, MA, USA. He has been a principal investigator on a number of research projects with the NASA Ames and Langley research centers, related to air traffic management. His research interests included decision support for air traffic management including airport surface operations, collaborative and distributed traffic flow management, and trajectory planning. He has over thirty related publications.

Ni Shen received a master of science in operations research (2009) and a Ph.D. in air transportation system engineering (2010), both from Virginia Tech, Blacksburg, VA, USA. She has been working as a Research Engineer at Engility Cooperation, Billerica, MA, USA since 2010. Her research interests include system modeling and simulation, and data analysis. Dr. Shen is a member of AIAA.